



# HHS Public Access

Author manuscript

*J Immunol.* Author manuscript; available in PMC 2016 March 15.

Published in final edited form as:

*J Immunol.* 2015 March 15; 194(6): 2635–2642. doi:10.4049/jimmunol.1402261.

## **<sup>1</sup> miR-182 is largely dispensable for adaptive immunity: lack of correlation between expression and function**

**Joseph N. Pucella<sup>\*</sup>, Wei-Feng Yen<sup>\*,†,¶</sup>, Myoungjoo V. Kim<sup>\*,†,¶</sup>, Joris van der Veecken<sup>\*,†,¶</sup>, Nicholas D. Socci<sup>‡</sup>, Yukiko Naito<sup>§</sup>, Ming O. Li<sup>\*,†</sup>, Naoharu Iwai<sup>§</sup>, and Jayanta Chaudhuri<sup>\*,†</sup>**

<sup>\*</sup>Immunology Program, Memorial Sloan Kettering Cancer Center, Gerstner Sloan-Kettering Graduate School, New York, New York, 10065

<sup>†</sup>Immunology and Microbial Pathogenesis Program, Weill-Cornell Graduate School of Medical Sciences, New York, New York, 10065

<sup>‡</sup>Bioinformatics Core, Memorial Sloan Kettering Cancer Center, New York, New York, 10065

<sup>§</sup>Department of Genomic Medicine, National Cerebral and Cardiovascular Center, Suita, Osaka, Japan

### **Abstract**

MicroRNA (miR)-mediated regulation of protein abundance is a pervasive mechanism of directing cellular processes. The well-studied and abundant miR-182 has previously been implicated in many aspects of T cell function, DNA repair and cancer. Here, we show that miR-182 is the most highly induced miR in B cells undergoing class switch recombination (CSR). To elucidate the requirement of miR-182 in lymphocyte function, we extensively characterized mice with a targeted deletion of *Mir182*. We show that despite its dramatic induction, loss of miR-182 has minimal impact on B cell development, the ability of B cells to undergo CSR *ex vivo* and to undergo antigen-driven affinity maturation *in vivo*. Furthermore, in striking contrast to knockdown studies that demonstrated the requirement of miR-182 in T cell function, miR-182 deficient mice display no defect in T cell development and activation. Finally, we show that T cell dependent immune response to experimental *Listeria monocytogenes* infection is intact in miR-182 deficient mice. We conclude that, contrary to previous studies, miR-182 does not play a significant role in all measured aspects of mouse adaptive immunity. This striking absence of a phenotype highlights the lack of correlation between expression pattern and functional requirement, underscores the limitations of using knockdown approaches to assess miR requirements, and suggests that miR networks may compensate for the chronic loss of specific miRs.

### **Introduction**

Mature IgM<sup>+</sup> B cells in secondary lymphoid organs such as the spleen and the lymph nodes undergo class switch recombination (CSR) to exchange the default C<sub>μ</sub> constant region exons for an alternate constant region gene segment (C<sub>γ</sub>, C<sub>ε</sub>, C<sub>α</sub>) (1). The B cell thus shifts from

<sup>1</sup>This work was supported by the National Institutes of Health Grant 1R01AI072194 and a Starr Cancer Consortium Grant to JC

Corresponding author: Jayanta Chaudhuri, Phone: 646-888-2357, [chaudhuj@mskcc.org](mailto:chaudhuj@mskcc.org).

<sup>¶</sup>These authors contributed equally to this work

expressing IgM to IgG, IgE or IgA, with each antibody isotype conferring a distinct effector function during an immune response (1). Mechanistically, CSR is a DNA deletion-recombination reaction occurring between repetitive switch (S) region DNA elements in the immunoglobulin heavy chain locus (*IgH*). Current models posit that the DNA deaminase AID (activation-induced cytidine deaminase) deaminates cytidines to uridines in S regions. Engagement of base excision and mismatch repair proteins at the deaminated residues generates DNA double strand breaks (DSBs) at acceptor and donor S regions. Synapsis and end-joining of complete CSR (1).

CSR proceeds through the deliberate introduction of DNA lesions and relies on subversion of faithful DNA repair so as to promote accumulations of DSBs and long-range (productive) versus intra-switch (abortive) recombination (2, 3). While obligatory intermediates for CSR, DSBs also constitute one of the most toxic lesions that can occur in a cell, causing either cell death or initiating oncogenic translocations (4, 5). Processes that regulate the activity of AID to generate DNA lesions have been extensively investigated, however the mechanisms that tip the delicate balance of DNA repair to mediate CSR while simultaneously suppressing genomic instability remain elusive (3, 6).

MicroRNAs (miRs) represent a class of small non-coding RNAs that influence gene expression post-transcriptionally via translational repression and/or mRNA degradation (7, 8). Over the past two decades, the prevalence and sway of miR-mediated regulation in diverse cellular processes has become increasingly apparent. However, elucidation of miR regulatory mechanisms is often challenging due in part to miRs commonly exhibiting slight effects on an array of targets. This characteristic has led to the conjecture that miRs are often involved in the fine-tuning of cellular processes by hitting multiple nodes within a pathway or among several pathways simultaneously (9, 10). Fine regulation is necessary in instances when even small deviations could be deleterious, and so fine-tuning may play a role in maintaining homeostasis or moderating transitions from one cell state to another. Such a regulatory mechanism would fit well with the transient subversion of DNA repair mechanisms during CSR (2, 3). We therefore hypothesized that miR-mediated regulation plays a role in balancing DNA repair to permit productive CSR.

In this study, we have identified miR-182 as the most highly induced miR in B cells stimulated to undergo CSR. miR-182 is a member of the miR-183~182 cluster encoding miR-96, miR-182 and miR-183, with miR-182 being implicated in many aspects of lymphocyte function, DNA repair and cancer progression. AntagomiR-mediated depletion experiments demonstrated a central role of miR-182 in IL-2 driven helper T cell-dependent immune response through the ability of the miR to regulate expression of the transcriptional factor Foxo1 (11). miR-182 was shown to be a key effector of the suppressor activity of regulatory T cells during an immune response (12). Expression of miR-182 has been associated with a wide variety of tumors including those originating in breast, lungs, thyroid and ovary (13–16). Finally, miR-182 has been implicated in directly regulating expression of BRCA1 and over 30 gene products that participate in BRCA1-dependent homologous recombination DNA repair (17, 18), suggesting miR-182 participates in fine-tuning of DNA DSB response. One such miR-182 target is the mRNA encoding 53BP1, a protein with a well-established role in the DNA repair phase of CSR (19–22). Studies implicating miR-182

not only in regulating lymphocyte development and function, but also DNA repair via multiple intra-pathway targets, in combination with our identification of miR-182 as the most highly induced miR in B cells undergoing CSR, prompted us to characterize mice with a targeted deletion of miR-182 (23). In striking contrast to published reports, we find that miR-182 is largely dispensable for all measured aspects of lymphocyte function.

## Materials & Methods

### Mice and B cell cultures

The generation of *Aicda*<sup>-/-</sup> and *Mir182*<sup>-/-</sup> mice has been described (23, 24). Wild-type (control) BALB/c mice and C57BL/6 were obtained from The Jackson Laboratories. Mouse colonies were maintained according to IACUC policies. The purification of naïve mature B cells and stimulation conditions to induce CSR have been described (25). IL-5 was used at a concentration of 6µg/mL in plasma cell differentiation experiments. CSR frequency was determined by flow cytometry (25).

### Small RNA sequencing

Small RNA library preparation and subsequent sequencing was performed by the MSKCC Genomics Core Laboratory using standard Illumina HiSeq protocol. Raw data was processed by the MSKCC Bioinformatics Core Laboratory.

### Real-time qPCR

All qPCR experiments were performed using the following components from Applied Biosystems (Life Technologies): TaqMan miRNA Reverse Transcription Kit (#4366596), TaqMan Universal Master Mix II, no UNG (#4427788), TaqMan miRNA Assays (#4427975: miR-182 ID 002599; miR-96 ID 000186; miR-183 ID 00269; snoRNA251 ID 001236). Data was normalized to snoRNA251. Data analysis was performed using the Comparative Ct method (26). Standard curve interpolation was used to determine the copy number of miR-182 in different cell types. A standard curve was generated by “spiking” 5'-phosphorylated miR-182 RNA oligonucleotide (miRBase.org) into *Mir182*<sup>-/-</sup> RNA samples over a range of dilutions.

### Bone Marrow Harvest

Bone marrow was flushed out with phosphate-buffered saline plus 0.25% FBS from femurs of 8–10 week old littermate or age-matched male mice.

### NP-CGG immunization

NP(30)-CGG (#N-5055D-5; Biosearch Technologies) was precipitated with 10% alum. 4–6 week old C57BL/6 WT and *Mir182*<sup>-/-</sup> mice were immunized intraperitoneally with 50µg on day 0 and boosted with 50µg on day 14. Serum was collected on days 0, 7, 14, and 21, and the mice were sacrificed on day 21. To analyze expression of miR-182 in B cells *in vivo*, mice were immunized intraperitoneally on day 0 with 100 µg alum-precipitated NP(20–29)-CGG and sacrificed on day 10.

## ELISA

Coating antibodies for binding IgM, IgG1, IgG2a, IgG2b, IgG3, and IgA were purchased from Southern Biotech (#1020-01, 1070-01, 1080-01, 1090-01, 1100-01, and 1040-01 respectively). Coating antibody for detecting IgE was purchased from BD Pharmingen (#553413). The following isotype standards were used to calculate absolute concentration values: IgM (#14-4752-81; eBioscience), IgG1 (#0102-01; Southern Biotech), IgG2a (#M5409; Sigma), IgG2b (#M5534; Sigma), IgG3 (#553486, BD Pharmingen), IgA (#553478; BD Pharmingen), IgE (#557080; BD Pharmingen). Secondary antibodies for detecting IgM, IgG1, IgG2a, IgG2b, IgG3, IgA, IgE were purchased from Southern Biotech (#1020-05, 1070-05, 1080-05, 1090-05, 1100-05, 1040-05, and 1130-05 respectively). BSA-conjugated NP(8) [#N-50501-10] and NP(30) [#N-5050H-10] were obtained from Biosearch Technologies. Plates were read at 450nm on a Biotek Synergy HT detector.

## Purification and stimulation of T cells

Naïve CD4 and CD8 T cells from peripheral lymphoid organs were sorted in a flow cytometer based on CD25<sup>-</sup>CD62L<sup>+</sup>CD44<sup>-</sup> cell surface expression. Cells were labeled with CellTrace Violet dye (#C34557; Invitrogen) according to manufacturer's protocol and activated *in vitro* using plate bound anti-CD3, soluble anti-CD28 and soluble IL-2 for 4 days. Dye dilution was measured using flow cytometry.

## *Listeria monocytogenes* infection and analysis

Mice were intravenously infected with  $5 \times 10^3$  CFU of *Listeria monocytogenes* expressing chicken ovalbumin (LM-OVA). Fluorescent-dye-labeled antibodies against cell surface markers TCR $\beta$ , CD4, CD8, and CD44 were purchased from eBiosciences. PE-conjugated K<sup>b</sup>/ova-tetramer was obtained from the Tetramer Core Facility at MSKCC. Cells were incubated with specific antibodies for 30 min on ice in the presence of 2.4G2 mAb to block Fc $\gamma$ R binding. To determine IFN $\gamma$  and TNF $\alpha$  expression, lymphocytes were stimulated with 5  $\mu$ g/ml of LLO<sub>190-201</sub> for CD4<sup>+</sup> T cells or 10 nM SIINFEKL peptide for CD8<sup>+</sup> T cells in the presence of GolgiStop (BD Biosciences) for 5 hrs at 37 °C. After stimulation, cells were incubated with cell surface antibodies, fixed and permeabilized, and stained with anti-IFN $\gamma$  and anti-TNF $\alpha$  (eBiosciences). All samples were acquired with an LSR II flow cytometer (Becton Dickinson) and data was analyzed with FlowJo software (TreeStar).

## Statistical analysis

P values were determined by two-tailed unpaired Student's t-test. P value < 0.05 was considered statistically significant. All error bars represent standard error (s.e.m.).

## Results

### miR-182 is strongly induced in B cells undergoing CSR

To identify miRs that are involved in tempering DNA repair to allow for the long range synapsis and incongruent ligation necessary for productive CSR, we isolated mature, naïve B cells from spleens of wild-type (WT) and AID-deficient (*Aicda*<sup>-/-</sup>) mice and generated miR expression profiles for their resting and activated states. *Ex vivo* activation of splenic B

cells was achieved with a combination of anti-CD40 plus IL-4. This approach was designed to identify miRs that are not just strongly induced upon activation, but whose induction is also AID-dependent. In doing so, we aimed to narrow our search to miRs that respond specifically to DNA damage caused by AID activity. We utilized a simple measure, which we called the fold-change ratio (FCR), to rank the disparity in fold-change induction upon activation between WT and *Aicda*<sup>-/-</sup> B cells. We thereby generated a list of 30 abundant miR candidates which exhibited FCR>1.5 or <0.667 (Fig. S1). miR-182 was identified as the most strongly induced miR upon B cell activation (Fig. 1A). There was an ~90-fold induction of miR-182 expression in WT B cells activated to undergo CSR. This induction was significantly dampened (to ~30-fold) in *Aicda*<sup>-/-</sup> B cells, suggesting that the enhanced induction could be dependent on AID-induced DNA breaks (Fig. 1A, inset). miR-182 is abundantly expressed, as it easily falls in the top 10% of expressed miRs in activated B cells and is readily quantifiable in activated lymphocytes (Fig. 1B, C). Additionally, normalized sequencing counts showed that miR-182 clusters with, and in most cases outnumbers, other miRs reported to play a role in B cell biology (27) (Fig. 1B, S1). The induction of miR-182 expression upon activation of B cells was also observed in independent qPCR analysis of *ex vivo* stimulated (Fig. 1D) and *in vivo* activated B cells (Fig. 1E). Since miR-182 has been strongly implicated in DNA repair, we extensively characterized B cells derived from mice with a targeted deletion of miR-182 (*Mir182*<sup>-/-</sup>) (23). miR-182 was not detected in B cells from *Mir182*<sup>-/-</sup> mice (Fig. 1D).

### miR-182 deficiency has minimal impact on B cell development, CSR and affinity maturation

Initially we characterized B cell development in *Mir182*<sup>-/-</sup> mice. Cell numbers in the bone marrow and spleen were similar between WT and *Mir182*<sup>-/-</sup> mice (Fig. 2A). No significant difference in the frequency of pro-, pre-, and immature B cell populations in the bone marrow was observed (Fig. 2B). Thus, early B cell development appears unaffected by absence of miR-182 and strongly suggests that V(D)J recombination, another process heavily reliant on DNA repair (28), remains intact. There was a statistically significant, albeit modest, decrease in the frequency of mature B cells (B220<sup>+</sup> CD43<sup>-</sup>) in total splenocyte populations from *Mir182*<sup>-/-</sup> mice (Fig. 2C). This difference was not reflected in the frequency of total (B220<sup>+</sup> IgM<sup>+</sup>) and mature (IgM<sup>lo</sup> IgD<sup>hi</sup>) B cells (Fig. 2C) suggesting that the slight reduction in percentage of B cells in spleen is due to a mild perturbation in the non-B cell population which could include T cells, macrophages, dendritic cells and other stromal cells. Furthermore, the frequencies of immature (IgM<sup>hi</sup> IgD<sup>lo</sup>), IgM<sup>hi</sup> IgD<sup>hi</sup>, T2-transitional (CD23<sup>+</sup> IgM<sup>+</sup> CD21<sup>hi</sup>), follicular (CD23<sup>+</sup> IgM<sup>+</sup> CD21<sup>lo</sup>), marginal zone (CD23<sup>-</sup> IgM<sup>hi</sup> CD21<sup>hi</sup>) and bone marrow recirculating (B220<sup>hi</sup> IgM<sup>+</sup>) B cell populations were all equivalent (Fig. 2C, D). There was a small but statistically significant decrease in the percentage of T1-transitional B cells (CD23<sup>-</sup> IgM<sup>hi</sup> CD21<sup>lo</sup>) in *Mir182*<sup>-/-</sup> mice (Fig. 2D). Overall, we conclude that B cell development is not impaired in *Mir182*<sup>-/-</sup> mice.

To determine the requirement of miR-182 in CSR, we stimulated splenic B cells *ex vivo* with anti-CD40 and IL-4 and assayed for CSR to IgG1. Despite the dramatic induction of miR-182 expression (Fig. 1), loss of miR-182 had no impact on the ability of B cells to undergo CSR to IgG1 (Fig. 2E). Likewise, splenic B cells from *Mir182*<sup>-/-</sup> mice cultured in

LPS underwent CSR to IgG3 at WT levels (Fig. 2F). Thus, loss of miR-182 had no effect on the intrinsic ability of B cells to undergo CSR in culture. Additionally, miR-182 did not influence the differentiation of activated B cells into antibody-secreting plasma cells as measured by surface expression of CD138 (Syndecan) following stimulation of splenic B cells with anti-CD40, IL-4 and IL-5 (Fig 2G).

To assess the participation of miR-182 in secondary diversification of B cells *in vivo*, we analyzed WT and *Mir182*<sup>-/-</sup> mice following immunization with the T cell-dependent antigen NP-CGG (Fig. 3A). The fraction of germinal center B cells (GL7<sup>+</sup> Fas<sup>+</sup>) in spleens of immunized WT and *Mir182*<sup>-/-</sup> mice was similar, and as expected (24), markedly lower than that from *Aicda*<sup>-/-</sup> mice (Fig. 3B, C). Analysis of serum of immunized mice failed to show any significant difference in immunization-dependent secretion of various antibody isotypes (Fig. 3D), indicating that *in vivo* CSR in response to NP-CGG was normal and further bolstering the claim that plasma cell differentiation does not rely on miR-182. Finally, to assess antigen-specific affinity maturation, we probed for low- and high-affinity NP-specific serum antibodies via the binding of NP(30)- and NP(8)-BSA, respectively. Both low-affinity (Fig. 3E) and high-affinity (Fig. 3F) NP-specific antibodies were generated at normal levels in *Mir182*<sup>-/-</sup> mice. Overall, the B cell-dependent immune response in *Mir182*<sup>-/-</sup> mice was typical, displaying no statistically significant differences with WT mice. While there may be a trend for slightly lowered production of some isotypes, the magnitude of the difference is unlikely to be biologically relevant. Importantly, the primary isotype induced by NP exposure, IgG1, is clearly produced at rates similar to WT counterparts. We conclude that miR-182 plays a minimal role, if any, in B cell development and B cell function during a primary response to a T cell-dependent antigen.

### miR-182 is dispensable for T cell development and activation

A significant body of work has evaluated the role of miR-182 in T cell function. Transient knockdown of miR-182 using antagomiR technology suggested it was critical in CD4<sup>+</sup> helper T cell activation, clonal expansion, and *in vivo* function (11, 12). A detailed examination of *Mir182*<sup>-/-</sup> mice revealed no significant differences in thymic and peripheral T cell populations.

The proportions of developing double negative CD4<sup>-</sup> CD8<sup>-</sup> (DN), double positive CD4<sup>+</sup> CD8<sup>+</sup> (DP), single positive CD4<sup>+</sup>/CD8<sup>+</sup> (SP) and mature CD4<sup>+</sup>/CD8<sup>+</sup> SP cells in the thymus (Fig 4A, B), as well as the fraction of mature CD4<sup>+</sup>/CD8<sup>+</sup> SP and T regulatory cells (T<sub>reg</sub>) in the periphery (Fig. 4C, D), was similar between WT and *Mir182*<sup>-/-</sup> mice, arguing against a role for miR-182 in T cell development.

To assess proliferation of T cells upon activation in culture, naïve splenic CD4 SP T cells from WT and *Mir182*<sup>-/-</sup> mice were stimulated *ex vivo* with anti-CD28, anti-CD3, and IL-2. Indeed, miR-182 was strongly induced upon activation of WT CD4<sup>+</sup> helper T cells, as well as CD8<sup>+</sup> cytotoxic T cells (Fig. 5A). However, there was no significant difference in viability (as assessed by live/dead staining) or proliferation (as measured by CellTrace dye dilution) of CD4 T cells upon activation (Fig. 5B, D), in direct contrast to results observed with transient knockdown (11). Likewise, no difference was found in viability and proliferation of cytotoxic T cells upon activation (Fig. 5C, E).



### In vivo systemic immune response does not require miR-182

To functionally test *in vivo* immune response to a pathogen, we infected WT and *Mir182*<sup>-/-</sup> mice with *Listeria monocytogenes* expressing LM-OVA antigen to induce a well-characterized systemic infection. CD4<sup>+</sup> and CD8<sup>+</sup> SP T cells were isolated from spleen and liver after 7 days (Fig. 6A). miR-182 was markedly induced upon *in vivo* activation of T cells infected with *L. monocytogenes* (Fig. 6B). It is noteworthy that although CD44<sup>+</sup> T cells can be detected in uninfected mice, robust induction of miR-182 in these cells occurs only upon infection (Fig. 6B). Sorted CD4<sup>+</sup> and CD8<sup>+</sup> SP T cells were restimulated *ex vivo* with listeriolysin O (LLO) or OVA-derived SIINFEKL peptide, respectively (Fig. 6A). No difference in effector cytokine production, as measured by the percentage of cells expressing intracellular IFN $\gamma$  and TNF $\alpha$ , was detected in both spleen and liver for CD4<sup>+</sup> SP (Fig. 6C) and CD8<sup>+</sup> SP (Fig. 6E) cells. Similarly, there was only minimal perturbation in the abundance and activation of OVA-specific cytotoxic T cells (Fig. 6D). Thus, *Mir182*<sup>-/-</sup> mice present no defect in the systemic immune response to *L. monocytogenes*. This contradicts previously published work that implicated miR-182 in promoting the *in vivo* function of helper T cells (11), though different approaches were used to test functional relevance.

### Discussion

Our results clearly demonstrate a striking lack of phenotype in a broad survey of the adaptive immune system in *Mir182*<sup>-/-</sup> mice. There is thus a remarkable lack of correlation between its expression pattern and role in B cells. This is contrary to the well-documented role of miR-155 in B cell development and CSR (29–31), even though induction of miR-155 is significantly less robust than that of miR-182 (Fig. 1). While miR-182 has been strongly implicated in DNA repair, it is evident that the repair modulatory activity is not relevant to either CSR or to suppression of lymphomagenesis as *Mir182*<sup>-/-</sup> mice are not tumor prone (data not shown). One explanation for the lack of a B cell defect is functional compensation by miR-183 and miR-96, both of which are expressed from a polycistronic transcript together with miR-182 and whose expression is not altered in either direction in *Mir182*<sup>-/-</sup> B cells (Fig. S3). Analysis of mice with deletion of this entire miR cluster could address the possibility of compensation.

The lack of phenotype in T cells is even more striking given that multiple reports have demonstrated a role of miR-182 in T cell function (11, 12). The failure to recapitulate observations derived from antagomiR-knockdown experiments could be due to off target effects of knockdown technology. But our results could also hint at an underappreciated malleability of miR networks upon long-term deprivation of one of its components. The potentially disparate biological consequences of acute and chronic miR deficiency beg careful reevaluation of published miR knockdown studies and consideration in future interpretations of miR modulation experiments.

### Supplementary Material

Refer to Web version on PubMed Central for supplementary material.

## Acknowledgments

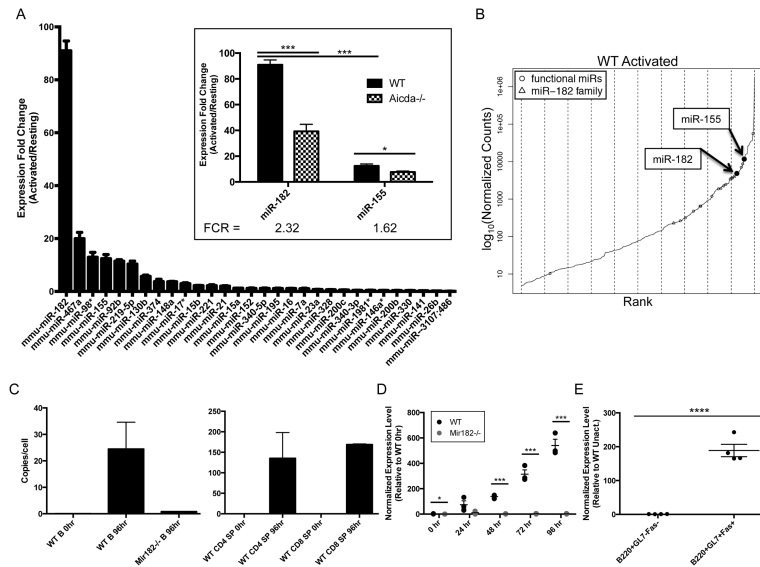
We thank members of the Chaudhuri laboratory for helpful discussions and suggestions. We also thank members of the Ventura, Rudensky and Li laboratories for technical and conceptual advice and Gaspare La Rocca for supportive discussions.

## References

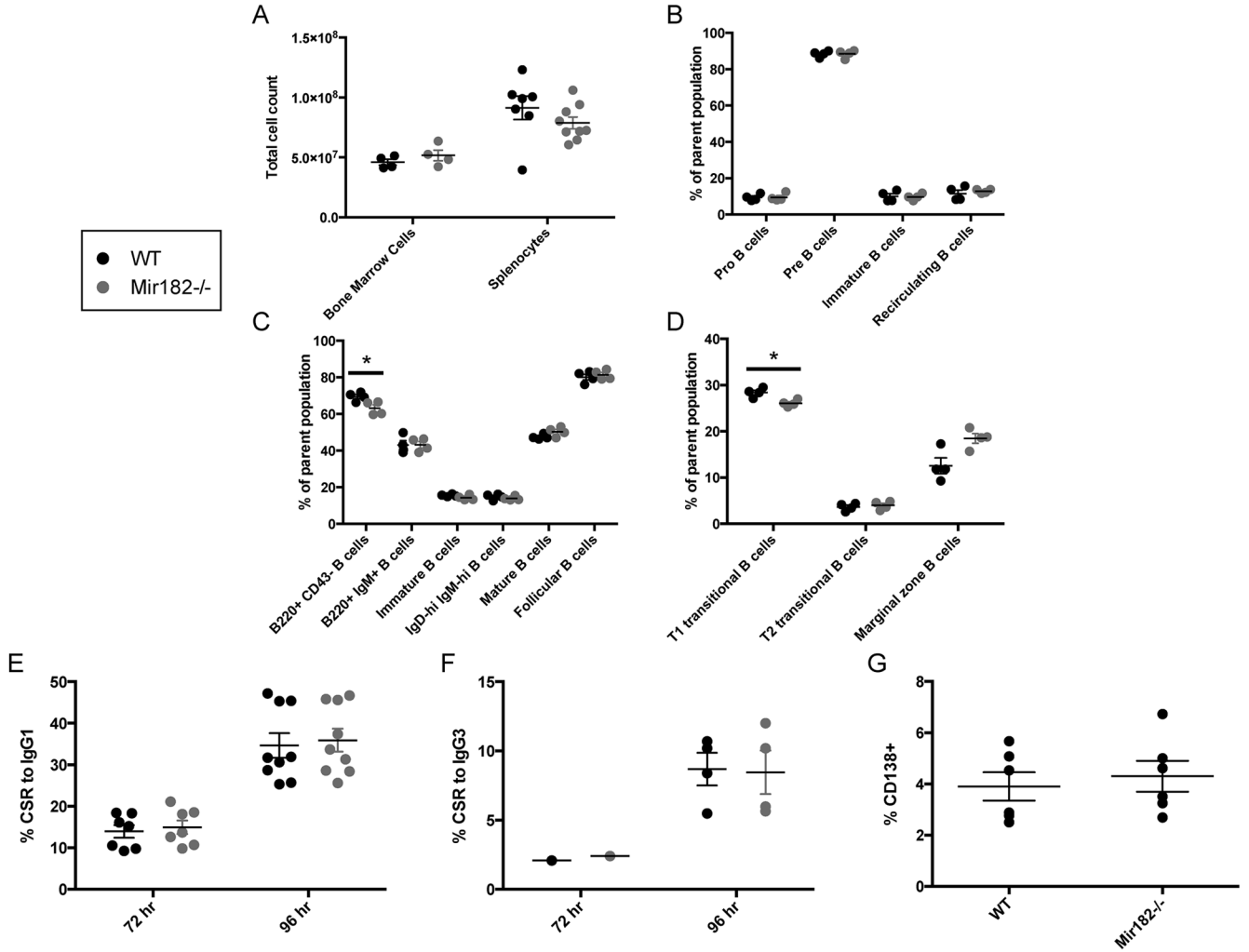
1. Stavnezer J. Complex regulation and function of activation-induced cytidine deaminase. *Trends Immunol.* 2011; 32:194–201. [PubMed: 21493144]
2. Liu M, Duke JL, Richter DJ, Vinuesa CG, Goodnow CC, Kleinstein SH, Schatz DG. Two levels of protection for the B cell genome during somatic hypermutation. *Nature.* 2008; 451:841–845. [PubMed: 18273020]
3. Matthews AJ, Zheng S, Dimenna LJ, Chaudhuri J. Regulation of immunoglobulin class-switch recombination: choreography of noncoding transcription, targeted DNA deamination, and long-range DNA repair. *Adv Immunol.* 2014; 122:1–57. [PubMed: 24507154]
4. Pasqualucci L, Bhagat G, Jankovic M, Compagno M, Smith P, Muramatsu M, Honjo T, Morse HC 3rd, Nussenzweig MC, Dalla-Favera R. AID is required for germinal center-derived lymphomagenesis. *Nat Genet.* 2008; 40:108–112. [PubMed: 18066064]
5. Nussenzweig A, Nussenzweig MC. Origin of chromosomal translocations in lymphoid cancer. *Cell.* 2010; 141:27–38. [PubMed: 20371343]
6. Keim C, Kazadi D, Rothschild G, Basu U. Regulation of AID, the B-cell genome mutator. *Genes Dev.* 2013; 27:1–17. [PubMed: 23307864]
7. Bartel DP. MicroRNAs: target recognition and regulatory functions. *Cell.* 2009; 136:215–233. [PubMed: 19167326]
8. Xiao C, Rajewsky K. MicroRNA control in the immune system: basic principles. *Cell.* 2009; 136:26–36. [PubMed: 19135886]
9. Lawrie CH. MicroRNAs in hematological malignancies. *Blood Rev.* 2013; 27:143–154. [PubMed: 23623930]
10. Loeb GB, Khan AA, Canner D, Hiatt JB, Shendure J, Darnell RB, Leslie CS, Rudensky AY. Transcriptome-wide miR-155 binding map reveals widespread noncanonical microRNA targeting. *Mol Cell.* 2012; 48:760–770. [PubMed: 23142080]
11. Stittrich AB, Haftmann C, Sgouroudis E, Kuhl AA, Hegazy AN, Panse I, Riedel R, Flossdorf M, Dong J, Fuhrmann F, Heinz GA, Fang Z, Li N, Bissels U, Hatam F, Jahn A, Hammoud B, Matz M, Schulze FM, Baumgrass R, Bosio A, Mollenkopf HJ, Grun J, Thiel A, Chen W, Hofer T, Loddenkemper C, Lohning M, Chang HD, Rajewsky N, Radbruch A, Mashreghi MF. The microRNA miR-182 is induced by IL-2 and promotes clonal expansion of activated helper T lymphocytes. *Nat Immunol.* 2010; 11:1057–1062. [PubMed: 20935646]
12. Kelada S, Sethupathy P, Okoye IS, Kistasis E, Czieso S, White SD, Chou D, Martens C, Ricklefs SM, Virtaneva K, Sturdevant DE, Porcella SF, Belkaid Y, Wynn TA, Wilson MS. miR-182 and miR-10a are key regulators of Treg specialisation and stability during Schistosome and Leishmania-associated inflammation. *PLoS Path.* 2013; 9:e1003451.
13. Wang L, Zhu MJ, Ren AM, Wu HF, Han WM, Tan RY, Tu RQ. A ten-microRNA signature identified from a genome-wide microRNA expression profiling in human epithelial ovarian cancer. *PloS One.* 2014; 9:e96472. [PubMed: 24816756]
14. Wang S, Yang MH, Wang XY, Lin J, Ding YQ. Increased expression of miRNA-182 in colorectal carcinoma: an independent and tissue-specific prognostic factor. *Int J Clinical Exp Path.* 2014; 7:3498–3503. [PubMed: 25031782]
15. Lei R, Tang J, Zhuang X, Deng R, Li G, Yu J, Liang Y, Xiao J, Wang HY, Yang Q, Hu G. Suppression of MIM by microRNA-182 activates RhoA and promotes breast cancer metastasis. *Oncogene.* 2014; 33:1287–1296. [PubMed: 23474751]
16. Segura MF, Hanniford D, Menendez S, Reavie L, Zou X, Alvarez-Diaz S, Zakrzewski J, Blochin E, Rose A, Bogunovic D, Polsky D, Wei J, Lee P, Belitskaya-Levy I, Bhardwaj N, Osman I, Hernando E. Aberrant miR-182 expression promotes melanoma metastasis by repressing FOXO3



- and microphthalmia-associated transcription factor. *Proc Natl Acad Sci USA*. 2009; 106:1814–1819. [PubMed: 19188590]
17. Moskwa P, Buffa FM, Pan Y, Panchakshari R, Gottipati P, Muschel RJ, Beech J, Kulshrestha R, Abdelmohsen K, Weinstock DM, Gorospe M, Harris AL, Helleday T, Chowdhury D. miR-182-mediated downregulation of BRCA1 impacts DNA repair and sensitivity to PARP inhibitors. *Mol Cell*. 2011; 41:210–220. [PubMed: 21195000]
  18. Krishnan K, Steptoe AL, Martin HC, Wani S, Nones K, Waddell N, Mariasegaram M, Simpson PT, Lakhani SR, Gabrielli B, Vlassov A, Cloonan N, Grimmond SM. MicroRNA-182–5p targets a network of genes involved in DNA repair. *RNA*. 2013; 19:230–242. [PubMed: 23249749]
  19. Bothmer A, Robbiani DF, Feldhahn N, Gazumyan A, Nussenzweig A, Nussenzweig MC. 53BP1 regulates DNA resection and the choice between classical and alternative end joining during class switch recombination. *J Exp Med*. 2010; 207:855–865. [PubMed: 20368578]
  20. Jankovic M, Feldhahn N, Oliveira TY, Silva IT, Kieffer-Kwon KR, Yamane A, Resch W, Klein I, Robbiani DF, Casellas R, Nussenzweig MC. 53BP1 Alters the Landscape of DNA Rearrangements and Suppresses AID-Induced B Cell Lymphoma. *Mol Cell*. 2013; 49:623–631. [PubMed: 23290917]
  21. Manis JP, Morales JC, Xia Z, Kutok JL, Alt FW, Carpenter PB. 53BP1 links DNA damage-response pathways to immunoglobulin heavy chain class-switch recombination. *Nat Immunol*. 2004; 5:481–487. [PubMed: 15077110]
  22. Ward IM, Reina-San-Martin B, Oлару A, Minn K, Tamada K, Lau JS, Cascalho M, Chen L, Nussenzweig A, Livak F, Nussenzweig MC, Chen J. 53BP1 is required for class switch recombination. *J Cell Biol*. 2004; 165:459–464. [PubMed: 15159415]
  23. Jin ZB, Hirokawa G, Gui L, Takahashi R, Osakada F, Hiura Y, Takahashi M, Yasuhara O, Iwai N. Targeted deletion of miR-182, an abundant retinal microRNA. *Mol Vision*. 2009; 15:523–533.
  24. Muramatsu M, Kinoshita K, Fagarasan S, Yamada S, Shinkai Y, Honjo T. Class switch recombination and hypermutation require activation-induced cytidine deaminase (AID), a potential RNA editing enzyme. *Cell*. 2000; 102:553–563. [PubMed: 11007474]
  25. Vuong BQ, Lee M, Kabir S, Irimia C, Macchiarulo S, McKnight GS, Chaudhuri J. Specific recruitment of protein kinase A to the immunoglobulin locus regulates class-switch recombination. *Nat Immunol*. 2009; 10:420–426. [PubMed: 19234474]
  26. Schmittgen TD, Livak KJ. Analyzing real-time PCR data by the comparative C(T) method. *Nat Protocols*. 2008; 3:1101–1108.
  27. Li J, Wan Y, Ji Q, Fang Y, Wu Y. The role of microRNAs in B-cell development and function. *Cellular Mol Immunol*. 2013; 10:107–112. [PubMed: 23314697]
  28. Schatz DG, Ji Y. Recombination centres and the orchestration of V(D)J recombination. *Nat Rev Immunol*. 2011; 11:251–263. [PubMed: 21394103]
  29. Dorsett Y, McBride KM, Jankovic M, Gazumyan A, Thai TH, Robbiani DF, Di Virgilio M, Reina San-Martin B, Heidkamp G, Schwickert TA, Eisenreich T, Rajewsky K, Nussenzweig MC. MicroRNA-155 suppresses activation-induced cytidine deaminase-mediated Myc-Igh translocation. *Immunity*. 2008; 28:630–638. [PubMed: 18455451]
  30. Teng G, Hakimpour P, Landgraf P, Rice A, Tuschl T, Casellas R, Papavasiliou FN. MicroRNA-155 is a negative regulator of activation-induced cytidine deaminase. *Immunity*. 2008; 28:621–629. [PubMed: 18450484]
  31. Vigorito E, Perks KL, Abreu-Goodger C, Bunting S, Xiang Z, Kohlhaas S, Das PP, Miska EA, Rodriguez A, Bradley A, Smith KG, Rada C, Enright AJ, Toellner KM, MacLennan IC, Turner M. microRNA-155 regulates the generation of immunoglobulin class-switched plasma cells. *Immunity*. 2007; 27:847–859. [PubMed: 18055230]

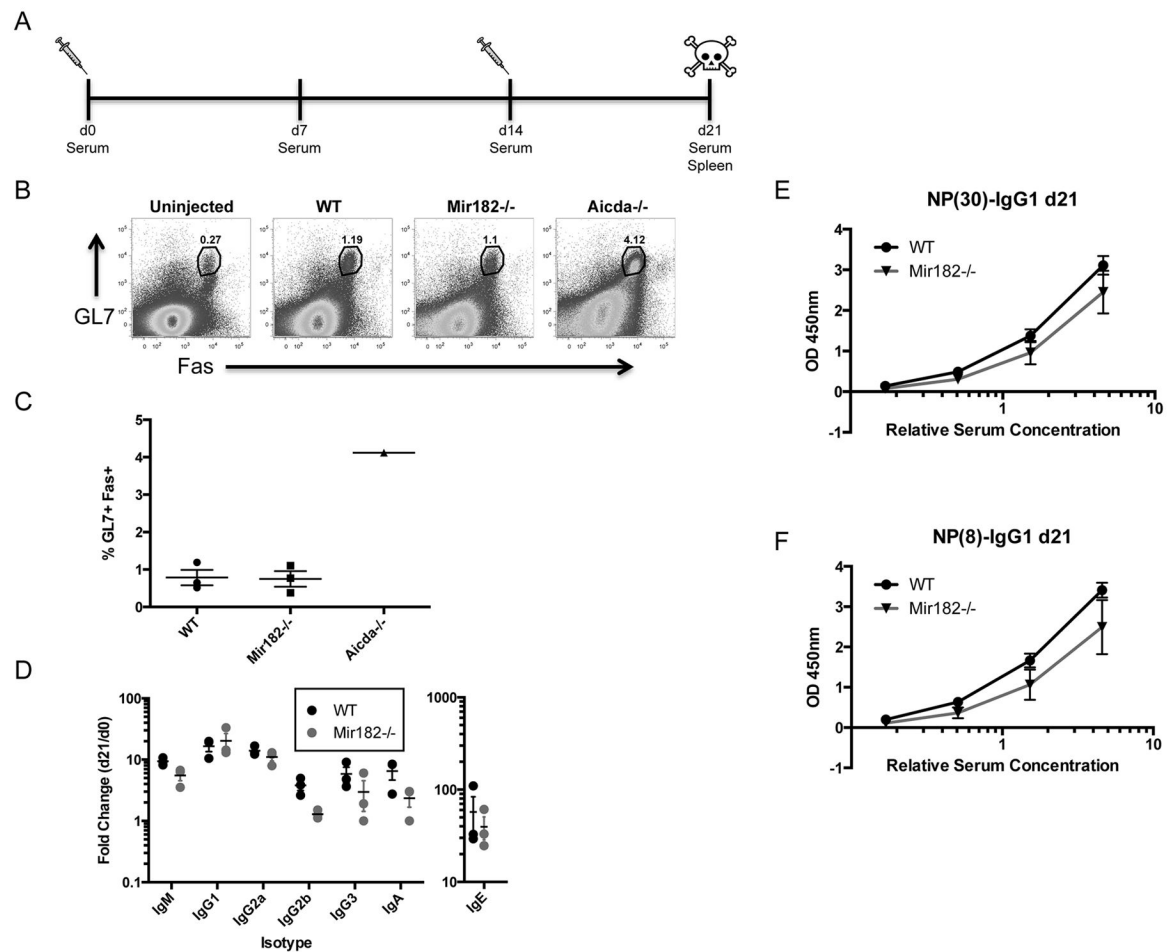


**FIGURE 1.** miR-182 is strongly induced upon B cell activation in an AID-dependent manner. **(A)** Expression fold-change of top 30 miR candidates in WT B cells (activated/resting) identified by miR expression profiling. n=3 **(Inset)** Expression fold-change of miR-182 and miR-155 (activated/resting). Fold-change ratio (FCR) = Fold-change WT/Fold-change *Aicda*<sup>-/-</sup>. **(B)** Normalized sequencing counts of all expressed miRs were ranked and plotted. Marked “functional miRs” refer to miRs in which there is published evidence citing a role in B cell development and/or function (27). **(C–E)** TaqMan qPCR was used to monitor expression of miR-182. **(C)** Approximate miR-182 absolute copy number was determined by interpolation on a standard curve generated using synthesized miR-182 RNA spiked into *Mir182*<sup>-/-</sup> RNA sample over a dilution series. n=3 for WT 96 hr samples, n=1 for other samples. **(D)** Mature splenic B cells were isolated and stimulated with anti-CD40 (0.5µg/mL) and IL-4 (12.5 ng/mL). n=3. **(E)** WT C57BL/6 mice immunized with NP(20–29)-CGG were sacrificed day 10 and indicated cell populations were FACS-sorted from splenocytes. \**p*<0.1, \*\*\**p*<0.001, \*\*\*\**p*<0.001 (t-test).

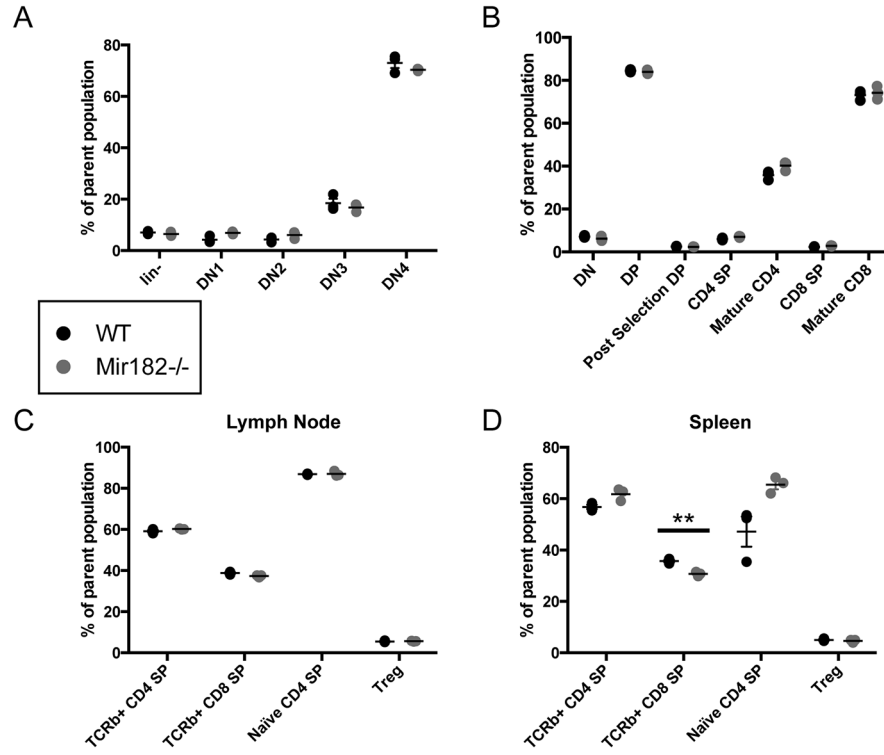


**FIGURE 2.**

B cell development and CSR are unperturbed by miR-182 deficiency. **(A)** Cellularity of bone marrow and spleen. **(B)** Bone marrow was analyzed for immature (B220<sup>lo</sup> IgM<sup>+</sup>) and recirculating (B220<sup>hi</sup> IgM<sup>+</sup>) B cells as a percentage of live singlets. B220<sup>lo</sup> IgM<sup>-</sup> B cells were gated and examined for Pro (CD43<sup>+</sup>) and Pre (CD43<sup>-</sup>) B cells. **(C, D)** Splenocytes were analyzed for relevant B cell populations. Parent population for B220<sup>+</sup> CD43<sup>-</sup> and B220<sup>+</sup> IgM<sup>+</sup> B cells is live singlets. Parent population for Immature (IgM<sup>hi</sup> IgD<sup>lo</sup>), IgM<sup>hi</sup> IgD<sup>hi</sup>, and Mature (IgM<sup>lo</sup> IgD<sup>hi</sup>) is B220<sup>+</sup> live singlets. Parent population for Follicular (IgM<sup>+</sup> CD21<sup>lo</sup>) and T2 transitional (IgM<sup>+</sup> CD21<sup>hi</sup>) B cells is B220<sup>+</sup> CD23<sup>+</sup> live singlets. Parent population for T1 transitional (IgM<sup>hi</sup> CD21<sup>lo</sup>) and Marginal zone (IgM<sup>hi</sup> CD21<sup>hi</sup>) B cells is B220<sup>+</sup> CD23<sup>-</sup> live singlets. **(E)** Primary mature splenic B cells were stimulated with anti-CD40 and IL-4 and assayed for surface IgG1 expression by flow cytometry. **(F)** Splenic B cells were stimulated with LPS and assayed for surface IgG3 expression by flow cytometry. **(G)** Splenic B cells were stimulated with anti-CD40, IL-4 and IL-5 and assayed for surface CD138 (Syndecan) expression by flow cytometry. \**p*<0.1 (t-test).

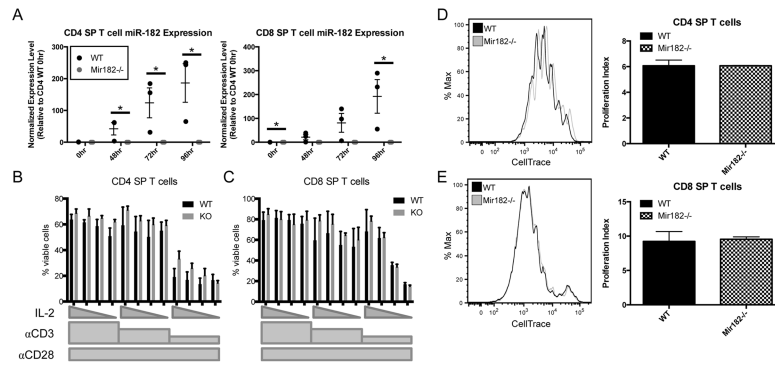
**FIGURE 3.**

Antigen-dependent primary B cell response is normal in *Mir182*<sup>-/-</sup> mice. (A) Schematic of NP-CGG immunization protocol with. (B) Abundance of germinal center B cells (GL7<sup>+</sup>Fas<sup>+</sup>) following NP-CGG immunization was assessed by flow cytometry. *Aicda*<sup>-/-</sup> mice, which have significantly higher germinal center B cells (24), were used as controls. (C) Quantification of germinal center B cells in immunized mice. (D) Fold-change in serum isotype concentrations upon NP-CGG immunization, determined by ELISA. (E–F) Detection of low-affinity (E) and high-affinity (F) NP-specific IgG<sub>1</sub> serum antibodies by ELISA.



**FIGURE 4.**

T cell development is unimpaired in *Mir182*<sup>-/-</sup> mice. (A–B) Thymic T cell populations observed by flow cytometry. (A) Parent population for  $lin^-$  is live singlets. Parent gate for DN1–4 is  $lin^-$ . Lin markers = CD19, CD4, CD8a, TCRβ, TCRγδ, CD11b, CD11c, Nk1.1, Ly6G(Gr1), Ter119. (B) Parent population for DN, DP, CD4 SP and CD8 SP is live singlets. Post-selection DP is % CD69<sup>+</sup> TCRβ<sup>+</sup> of CD4<sup>+</sup> CD8<sup>+</sup> live singlets. Mature CD4/CD8 SP is % CD69<sup>-</sup> CD62L<sup>+</sup> of CD4<sup>+</sup>/CD8<sup>+</sup> SP live singlets. (C–D) Analysis of peripheral T cell populations from lymph nodes (C) or spleen (D). Parent population for CD4/CD8 SP is live singlets. TCRβ<sup>+</sup> DN/DP/CD4 SP/CD8 SP is % DN/DP/CD4<sup>+</sup> SP/CD8<sup>+</sup> SP of TCRβ<sup>+</sup> live singlets. Naïve CD4 SP is % CD62L<sup>+</sup> CD44<sup>-</sup> of CD4<sup>+</sup> SP live singlets. Treg is % CD25<sup>+</sup> CD44<sup>-</sup> of CD4<sup>+</sup> SP live singlets.

**FIGURE 5.**

T cell activation is normal in *Mir182*<sup>-/-</sup> mice. **(A)** Sorted naïve splenic SP T cells were isolated from indicated mice and stimulated with plate-bound anti-CD3 (1 μg/mL), soluble anti-CD28 (4 μg/mL) and soluble IL-2 (1 U/mL) and TaqMan qPCR was used to monitor expression of miR-182. **(B, C)** Sorted naïve splenic SP T cells were isolated from indicated mice and stimulated with plate-bound anti-CD3 (10, 1, or 0.2 μg/mL), soluble anti-CD28 (2 μg/mL) and soluble IL-2 (50, 25, 10, or 1 U/mL). Bar graphs depict % viability for CD4<sup>+</sup>/CD8<sup>+</sup> SP T cells over stimulation conditions used. **(D)** Histogram overlay depicts representative CellTrace dilution profiles of CD4<sup>+</sup> SP T cells stimulated with anti-CD3 (1 μg/mL), anti-CD28 (2 μg/mL) and IL-2 (1 U/mL). Representative proliferation index for same stimulation conditions is shown. **(E)** Histogram overlay depicts representative CellTrace dilution profiles of CD8<sup>+</sup> SP T cells stimulated with anti-CD3 (10 μg/mL), anti-CD28 (2 μg/mL) and IL-2 (10 U/mL). Representative proliferation index for CD8<sup>+</sup> SP T cells stimulated with anti-CD3 (1 μg/mL), anti-CD28 (2 μg/mL) and IL-2 (25 U/mL) is shown. **(A–E)** n=3, \**p*<0.1 (t-test). **(B–E)** Data representative of 2 experiments.



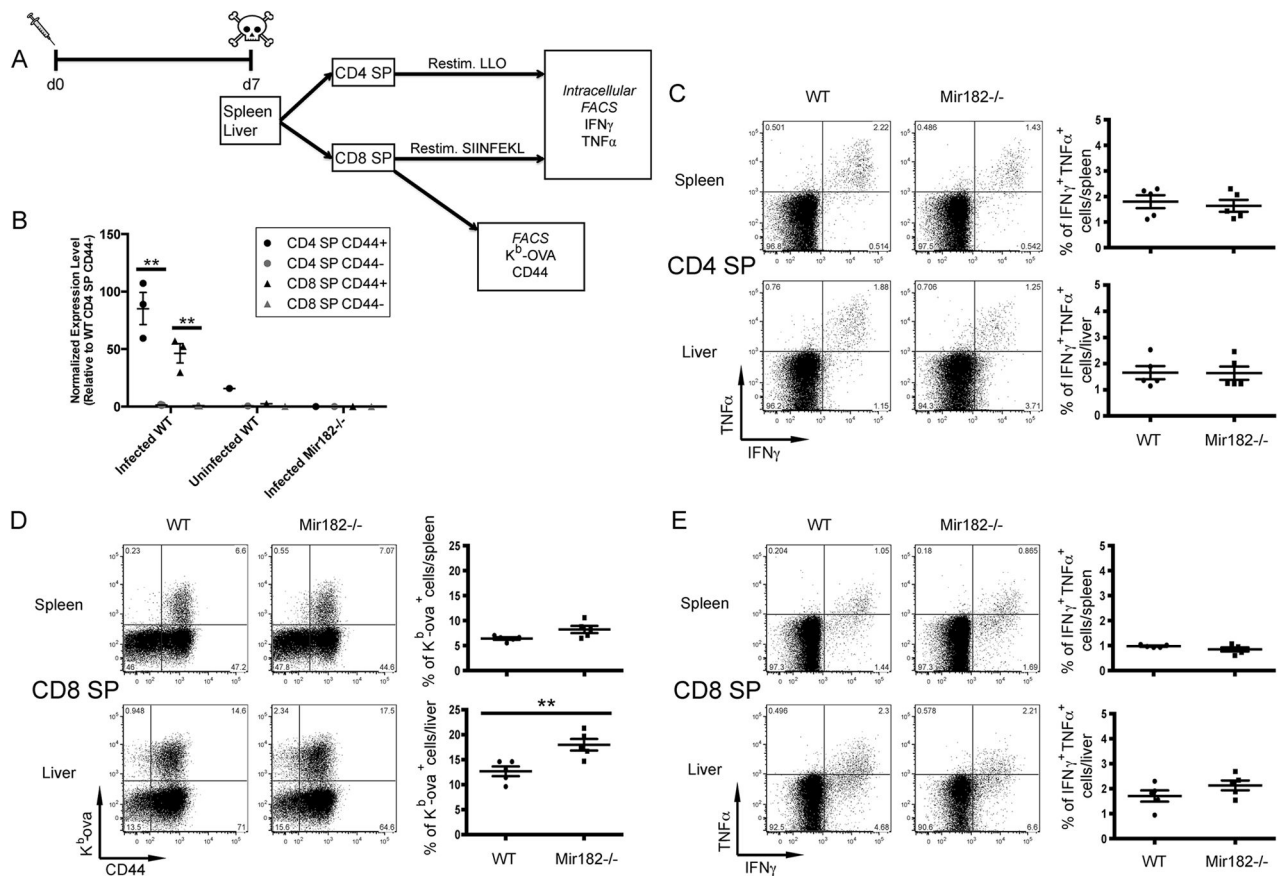


**FIGURE 6.** miR-182 deletion does not impair immune response to *Listeria monocytogenes*. **(A)** Schematic for intravenous infection with *Listeria monocytogenes*-OVA and subsequent analysis. **(B)** WT and *Mir182*<sup>-/-</sup> mice were infected with *L. monocytogenes* and sacrificed on day 7. Indicated cell populations were FACS-sorted from splenocytes and analyzed for miR-182 expression by TaqMan qPCR. \*\**p* < 0.01 (t-test) **(C)** Indicated cells were restimulated *ex vivo* with LLO peptide for 3 hours then analyzed by flow cytometry for intracellular effector cytokines. **(D)** Indicated cells were analyzed for surface expression of CD44 and OVA-specific TCR $\beta$ . **(E)** Indicated cells were restimulated *ex vivo* with SIINFEKL peptide for 3 hours then analyzed by flow cytometry for intracellular effector cytokines. **(C–E)** \*\**p* < 0.01 (Mann-Whitney test).